Cross Talk between Tetanus Neurotoxin-insensitive Vesicle-associated Membrane Protein-mediated Transport and L1-mediated Adhesion □□

Philipp Alberts,* Rachel Rudge,* Ina Hinners,† Aude Muzerelle,‡ Sonia Martinez-Arca,* Theano Irinopoulou,* Véronique Marthiens,§ Sharon Tooze,† Fritz Rathjen,‖ Patricia Gaspar,‡ and Thierry Galli*¶

*Membrane Traffic and Neuronal Plasticity, Institut National de la Santé et de la Recherche Médicale U536, F-75005 Paris, France; †Secretory Pathways Laboratory, Cancer Research UK, London Research Institute, London WC2A 3PX, United Kingdom; ‡Institut National de la Santé et de la Recherche Médicale U106, Hôpital Salpêtrière, F-75651, Paris, France; §Institut National de la Santé et de la Recherche Médicale U440, F-75005 Paris, France; and ‖Max-Delbrueck-Centrum fuer Molekulare Medizin, D-13092 Berlin, Germany

The membrane-trafficking pathway mediated by tetanus neurotoxin-insensitive vesicle-associated membrane protein (TI-VAMP) in neurons is still unknown. We show herein that TI-VAMP expression is necessary for neurite outgrowth in PC12 cells and hippocampal neurons in culture. TI-VAMP interacts with plasma membrane and endosomal target soluble *N*-ethylmaleimide-sensitive factor attachment protein receptors, suggesting that TI-VAMP mediates a recycling pathway. L1, a cell-cell adhesion molecule involved in axonal outgrowth, colocalized with TI-VAMP in the developing brain, neurons in culture, and PC12 cells. Plasma membrane L1 was internalized into the TI-VAMP–containing compartment. Silencing of TI-VAMP resulted in reduced expression of L1 at the plasma membrane. Finally, using the extracellular domain of L1 and N-cadherin immobilized on beads, we found that the silencing of TI-VAMP led to impaired L1- but not N-cadherin–mediated adhesion. Furthermore, TI-VAMP- but not synaptobrevin 2-containing vesicles accumulated at the site of the L1 bead-cell junction. We conclude that TI-VAMP mediates the intracellular transport of L1 and that L1-mediated adhesion controls this membrane trafficking, thereby suggesting an important cross talk between membrane trafficking and cell-cell adhesion.

INTRODUCTION

The development of the brain depends on the differentiation of neurons and particularly on the extension, branching, and connection of their axons and dendrites (Prochiantz, 1995). The outgrowth of axons and dendrites requires massive transport of lipids and proteins from the Golgi apparatus to these extensions of the plasma membrane, but the underlying molecular mechanism is largely unknown (Futerman and Banker, 1996). Neurite outgrowth also depends on the recycling of plasma membrane proteins, particularly cell substrate adhesion molecules (CAMs) such as integrins and CAMs of the immunoglobulin superfamily (IgCAMs) (Ka-

miguchi and Lemmon, 2000a). Current knowledge indicates that the exocytosis mediating neurite outgrowth differs from the exocytosis mediating neurotransmitter release, suggesting that separate subcellular and molecular pathways underlie each process. Syntaxin (Stx) 1, synaptosomal-associated protein 25 kd (SNAP25), and synaptobrevin 2 (Syb 2), the components of the synaptic soluble *N*-ethylmaleimide-sensitive factor attachment protein receptor (SNARE) complex, mediate the fusion of synaptic vesicles with the plasma membrane (for review, see Galli and Haucke, 2001). Accordingly, genetic ablation of SNAP25 leads to a blockade of evoked neurotransmitter release (Washbourne *et al.*, 2002), and Syb 2 genetic inactivation causes an almost complete loss of spontaneous and evoked release (Schoch *et al.*, 2001). However, the development of the brain seems normal in both Syb 2 and SNAP25 knockout mice (Schoch *et al.*, 2001; Washbourne *et al.*, 2002), indicating that these molecules are not necessary for neurite outgrowth. Similar results were also obtained in the case of Munc-18, an important regulator of syntaxin 1 (Verhage *et al.*, 2000). Furthermore, clostridial neurotoxins that cleave Syb have no effect on the development of neurons in culture (Osen-Sand *et al.*, 1996; Grosse *et al.*, 1999). However, former data have reported that botulinum neurotoxins that cleave SNAP25 do inhibit neurite outgrowth (Osen-Sand *et al.*, 1996). This discrepancy with

the findings in the SNAP25 knockout mouse could be owing to the expression of SNAP23, a close homolog that may be able to functionally replace SNAP25. In any case, these results clearly indicate that the molecules involved in the membrane-trafficking pathway mediating neurite outgrowth are, to a large extent, different from those involved in neurotransmitter release.

The finding that neurite outgrowth and apical transport in epithelial cells are insensitive to tetanus neurotoxin led us to investigate the function of tetanus neurotoxin-insensitive vesicle-associated membrane protein (TI-VAMP) (Galli *et al.*, 1998). We previously found that TI-VAMP defines a novel compartment, particularly enriched at the tip of growth cones in developing neurons (Coco *et al.*, 1999). TI-VAMP shows the same general structure as classical VAMPs, i.e., a SNARE motif, a carboxy-terminal transmembrane domain, and a short lumenal domain, but in addition carries an amino-terminal extension called the Longin domain (Filippini *et al.*, 2001). This domain inhibits the SNARE motif from interacting with cognate SNARE complexes both in vitro and in vivo (Martinez-Arca *et al.*, 2000, 2003b). Expression of the Longin domain of TI-VAMP results in strong inhibition of neurite outgrowth in PC12 cells (Martinez-Arca *et al.*, 2000) and both axonal and dendritic outgrowths in neurons in culture (Martinez-Arca *et al.*, 2001).

These results prompted us to further characterize the vesicular compartment containing TI-VAMP and its function in neurons. We show herein that TI-VAMP is essential for neurite outgrowth and interacts with plasma membrane and endosomal t-SNAREs. We found that L1, a cell-cell adhesion molecule involved in axonal outgrowth (Brummendorf *et al.*, 1998) and cell motility (Mechtersheimer *et al.*, 2001) colocalized with TI-VAMP in the developing brain, neurons in culture, and PC12 cells. Using the extracellular domain of L1 and N-cadherin immobilized on beads, we found that the silencing of TI-VAMP led to impaired L1- but not N-cadherin–mediated adhesion and that TI-VAMP–containing vesicles accumulated at the site of the L1 bead-cell junction. Therefore, our results demonstrate a cross talk between TI-VAMP–mediated transport and L1-mediated adhesion.

MATERIALS AND METHODS

Antibodies, Clones, and Reagents

The mouse monoclonal antibody (mAb) (clone 158.2) directed against TI-VAMP has been described elsewhere (Muzerelle *et al.*, 2003). Polyclonal anti-green fluorescent protein (GFP) antibody was described previously (Martinez-Arca *et al.*, 2001). Mouse monoclonal antibodies directed against Syb 2 (clone 69.1) and syntaxin 1 (HPC-1) and the polyclonal antibody against syntaxin 7 were generous gifts from R. Jahn (Max Planck Institute, Goettingen, Germany), C. Barnstable (Yale University, New Haven, CT), and Dr. W. Hong (Institute of Molecular and Cell Biology, Singapore, Republic of Singapore), respectively. Polyclonal rabbit antibodies against mouse L1 and Fab fragments generated from this antibody were described previously (Rathjen and Rutishauser, 1984). The polyclonal anti-Syb 2 antibody (MC23) was described previously (Chilcote *et al.*, 1995). The following commercial antibodies were used in this study: monoclonal anti-Na/K-ATPase a-1 (clone C464.6) from Upstate Biotechnology (Charlottesville, VA), monoclonal anti-syntaxin 13 (clone 15G2) from StressGen (San Diego, CA), and monoclonal anti-Vti1b (Transduction Laboratories clone 7) from BD Biosciences (Franklin Lakes, NJ). Affinity-purified Alexa 488 and Cy3-coupled goat anti-rabbit and anti-mouse immunoglobulins were from Jackson Immunoresearch Laboratories (West Grove, PA). Horseradish peroxidase- and alkaline phosphatase-coupled streptavidin, sheep anti-mouse and anti-rabbit IgGs were from Promega (Madison, WI). Nerve growth factor (NGF) was supplied by Alomone Labs (Rehovot, Israel). All other reagents were from Sigma-Aldrich (Saint Quentin Fallavier, France) unless specified.

DNA Constructions

The cDNA coding for L1-Fc chimera has been described previously (De Angelis *et al.*, 1999). Expression vectors coding for GFP and TI-VAMP fused to GFP have been described previously (Martinez-Arca *et al.*, 2000).

Cell Culture

PC12 cells were cultured and plated on collagen-coated glass coverslips as described previously (Martinez-Arca *et al.*, 2000). Cortical and striatal neurons were prepared from rat E16 embryos as described previously (Rousselet *et al.*, 1990). Hippocampal neurons from E18 rat brain were prepared as described previously (Chang and De Camilli, 2001). Purification of L1-Fc chimera was performed as described previously (De Angelis *et al.*, 1999). Briefly, Cos-7 cells were transiently transfected with cDNA coding for L1-Fc chimera by using LipofectAMINE-2000. Secreted L1-Fc protein was allowed to accumulate for several days in Ig-free medium. The supernatant was collected and recombinant protein was purified using protein A-Sepharose. To coat coverslips with L1-Fc chimera, coverslips were incubated for 2 h at 37°C with 20 μg/ml goat anti-human Fc-specific antibody (Sigma, Saint Quentin Fallavier, France) in Leibovitz medium, pH 8 (Invitrogen, Cergy Pontoise, France). Coverslips were rinsed and incubated with 3 μg/ml L1-Fc fragment in Leibovitz medium for another 2 h at 37°C.

Small Interfering Double-Stranded RNA (siRNA) Treatment of PC12 Cells

PC12 cells grown on collagen-coated 35-mm dishes were transfected by using 10 μl LipofectAMINE-2000 twice on two consecutive days with 0.5 μg of GFP plus either 4 μg of siRNA molecules corresponding to the rat TI-VAMP sequence, base pairs 486–506: AACCTCGTAGATTCGTCCGTC (siRNAr; Dharmacon, Lafayette, CO) or control siRNA molecules corresponding to the equivalent sequence of canine TI-VAMP: AATCTTGTGGATTCGTCTGTC (siRNAd; Proligo-Genset, Paris, France). The canine TI-VAMP sequence was obtained by reverse transcription-polymerase chain reaction of RNA from Madin-Darby canine kidney cells. The next day, cells were split and aliquots cultured on either collagen-coated coverslips or put back on collagen-coated culture dishes. For the neurite outgrowth assay, the cells were differentiated by the addition of 100 nM staurosporine 48 h after the second transfection, fixed the next day (i.e., 96 h after the first transfection), and processed for immunofluorescence with anti-GFP and anti-TI-VAMP antibodies. Thirty randomly chosen images for each condition were taken based on the GFP signal with a MicroMax charge-coupled device (CCD) camera (Princeton Instruments, Princeton, NJ), resulting in the analysis of at least 50 GFP-positive cells. A neurite was defined as a thin process >10 μm long. The length of each neurite, from the cell body limit until the tip of the process, was measured in each case by using MetaMorph software (Princeton Instruments). Differences were evaluated statistically with the chi square test. All the recordings and the MetaMorph analysis were done blind.

siRNA Treatment of Hippocampal Neurons

Neurons were dissected as described and plated on poly-D-lysine–coated 14-mm coverslips at a density of 25,000 cells/coverslip (16,500 cell/cm²). Four hours after plating, the media were replaced with neurobasal media plus 4% B27, and cells were transfected with 0.25 μg of GFP alone or cotransfected with 0.8 μg of siRNAr or siRNAd by using 0.5 μl of LipofectAMINE 2000. Four hours after transfection, the media were changed again to prevent any toxic effects of the LipofectAMINE. Neurons were transfected for a second time 24 h after plating; again, the media were replaced 4 h after transfection. Three days after dissection, neurons were fixed and processed for immunofluorescence with anti-GFP and anti-TI-VAMP antibodies. Transfected cells from three independent experiments were imaged with a MicroMax CCD camera (Princeton Instruments), resulting in the analysis of >75 neurons for each of the control conditions and >150 neurons treated with siRNAr. Neurite outgrowth measurements and statistical analysis were performed as described above.

Antibody Uptake Assay

PC12 cells were plated on collagen-coated glass coverslips and treated with NGF at a concentration of 50 ng/ml for 2–3 d. Cells were incubated with Fab fragments directed against L1 in NGF-containing medium at a concentration of 25 μg/ml for 60 min at 37°C. The cells were fixed after washes in cold phosphate-buffered saline with 1 mg/ml bovine serum albumin (BSA) and acid stripping with 0.2 M acetic acid/0.5 M NaCl for 2 min at 4°C. Antibody uptake on neurons grown on collagen-coated glass coverslips was performed essentially as described for PC12 cells. No acid stripping was performed, but after removal of Fab fragments and two washes of the cells in medium, neurons were reincubated for 60 min at 37°C.

Immunocytochemistry

Developmental localization of TI-VAMP and L1 was analyzed in Sprague-Dawley rats. Embryos (E13, E15, and E19) were extracted from timed preg-

nant dams after chloral hydrate anesthesia (E0, day of mating) and fixed in 4% paraformaldehyde overnight. After 24-h cryoprotection in 10% sucrose in phosphate buffer, serial cryostat sections (15 μm in thickness) were taken from the whole head in the sagittal plane for embryos. Sections were incubated overnight at room temperature in TI-VAMP mAb (clone 158.2; 1/500) alone or in combination with the L1 antibody (1/500) and processed for immunofluorescence.

Cells in culture were fixed with 4% paraformaldehyde/4% sucrose and processed for immunofluorescence as described previously (Coco et al., 1999). Optical conventional fluorescence microscopy was performed on a Provis microscope (Olympus, Tokyo, Japan) equipped with a MicroMax CCD camera (Princeton Instruments). Confocal laser scanning microscopy was performed using a SP2 confocal microscope (Leica Microsystems, Mannheim, Germany). Images were assembled using Adobe Photoshop (Adobe Systems, San Jose, CA).

Quantification of surface L1 signal was performed with a semiautomatic program based on the MetaMorph software (Universal Imaging, Downingtown, PA). Cells were segmented automatically, and the mask obtained by the segmentation procedure was used to compute the average intensity of the fluorescence over each cell. All acquisition and segmentation parameters were kept constant for all images. Differences were evaluated statistically with the Mann-Whitney nonparametric test.

Immunoprecipitation

Immunoprecipitation from rat brain was performed as described previously (Martinez-Arca et al., 2000). Monoclonal anti-TI-VAMP antibody 158.2 and control mouse IgG were covalently coupled to protein G-Sepharose according to Harlow and Lane (1988). Rat brain lysate was incubated with immunobeads overnight, and the beads were washed five times in homogenization buffer with 0.1% Triton X-100. Bound material was separated by SDS-PAGE (Schagger and von Jagow, 1987) followed by Western blotting.

Subcellular Fractionation

PC12 cells were homogenized with an EMBL-cell cracker in 10 mM HEPES-KOH pH 7.2, 250 mM sucrose, 1 mM EDTA, 1 mM MgOAc, and protease inhibitors. The homogenate was centrifuged at $800 \times g$ for 10 min, and 1.5 ml of the supernatant was loaded onto a 0.3–1.2 M linear sucrose gradient and spun for 15 min in a SW40 rotor at 25,000 rpm (velocity gradient). Then, 1-ml fractions were unloaded from the top; membranes were pelleted and resuspended in sample buffer. Equal volumes of each fraction were separated by SDS-PAGE (Laemmli, 1970) and analyzed by Western blotting. For equilibrium gradient analysis the light fractions 1–4 of the velocity gradient were pooled and loaded on a sucrose step gradient of the following composition: 1 ml 0.8 M, 2 ml 1 M, 2 ml 1.2 M, 2 ml 1.4 M, and 1 ml 1.6 M. After centrifugation in SW40 at 25,000 rpm overnight, the gradient was unloaded and analyzed as described above.

Rat brain was homogenized as described above. The supernatant (S1) was recentrifuged for 15 min at $9250 \times g$ to yield a supernatant (S2) and pellet (P2). The S2 fraction was further separated by velocity gradient centrifugation. An aliquot was loaded on top of a sucrose gradient ranging from 0.32 to 1.2 M sucrose and spun for 20 min at 25,000 rpm in a SW41 rotor. The gradient was unloaded by upward displacement, and 1-ml fractions were collected and the membranes were pelleted and resuspended in equal volumes of sample buffer. Equal volumes of each fraction were analyzed by SDS-PAGE and Western blotting. The first two fractions of the velocity gradient were further analyzed by equilibrium gradient centrifugation. The fractions were adjusted to a sucrose concentration of 0.6 M sucrose and mixed with 1.4 M sucrose to yield a linear gradient ranging from 0.6 to 1.4 M sucrose. Samples were spun overnight at 25,000 rpm in a SW41 rotor. Gradients were unloaded as described above. The membranes were pelleted and resuspended in equal volumes of sample buffer, and analysis was performed as described above.

Bead-Cell Adhesion Assay

Bead adhesion to PC12 cells was performed essentially as described previously (Lambert et al., 2000). For coating of L1-Fc chimera, surfactant-free latex-sulfate microspheres (diameter 6.2 μm for PC12 cells and 4 μm for hippocampal neurons; Interfacial Dynamics, Portland, OR) were incubated with goat anti-human Fc antibody (Sigma) at a ratio of 1 volume of IgGs/9 volumes of beads overnight at 4°C in 0.1 M borate buffer pH 8. Beads were then blocked with borate buffer containing 1% BSA for 15 min at room temperature in the case of PC12 cells or with BlockAid (Molecular Probes, Leiden, The Netherlands) in the case of hippocampal neurons. Blocked beads were incubated with L1-Fc (80 μg/ml) at a ratio of 1 volume of L1-Fc/4 volumes of beads in borate/BSA buffer for 2 h at room temperature or with borate/BSA buffer alone (control beads). For hippocampal neurons, beads were incubated with either L1-Fc fragment or with recombinant human Fc fragment at the same concentration (Jackson Immunoresearch Laboratories). For coupling N-cadherin-Fc chimera to beads, anti-mouse Fc antibodies were used (Jackson Immunoresearch Laboratories).

To test bead-cell adhesion, PC12 cells were seeded on collagen-coated coverslips (diameter 12 mm) at intermediate density. The next day, beads were added to the cells (2 μl of beads in 200 μl of complete medium) and left for 45 min at 37°C. Cells were washed with 3 ml of prewarmed medium, fixed, and analyzed by immunofluorescence. Neurons were plated at a density of 2×10^4 cells/14-mm coverslip and incubated with beads at day 3 in vitro in neurobasal media plus 4% B27 containing 1% BSA.

To test the role of TI-VAMP in L1 or N-cadherin–mediated bead-cell junctions, PC12 cells were treated with siRNA as described above. The bead-cell adhesion assay was performed as described above, and cells were stained with 158.2 and anti-L1-polyclonal antibody. For L1 beads images were acquired by conventional epifluorescence at a magnification of 40×. The choice of cells was based exclusively on the 158.2 signal, thus blind for the signal corresponding to cell-associated L1 beads. N-Cadherin beads were detected with anti-mouse Cy3-conjugated secondary antibody. In that case, choice of cells was based on the L1 signal thus blind for cell associated cadherin beads. The number of beads in each image was counted and differences were evaluated statistically with the Mann-Whitney nonparametric test.

The immunofluorescence intensities of the staining for TI-VAMP and Syb 2 in growth cones contacting an L1-coated bead were quantified using the "Region Measurement" function of the MetaMorph software (Universal Imaging). Growth cones were chosen on the basis of TI-VAMP signal thus blind for synaptorevin 2 signal. The average pixel intensity was computed over identical regions of identical basal and apical confocal sections for the TI-VAMP and Syb 2 signals. Differences were evaluated statistically with the Mann-Whitney nonparametric test.

Videomicroscopy

PC12 cells were transiently transfected with TI-VAMP-GFP by using LipofectAMINE 2000. The next day cells were incubated with L1- or N-cadherin beads in an appropriate chamber equilibrated to 37°C and 5% CO_2. TI-VAMP-GFP–positive cells with associated bead were recorded every 10 s (exposure time 300 ms) over a time period of 20 min by using a Leica DMIRE2 microscope equipped with a Cascade camera (Roper Scientific, San Antonio, TX).

Online Supplemental Material

The videos available in the online version correspond to the video stills shown in Figure 8B. PC12 cells expressing TI-VAMP-GFP were incubated with either L1-coated beads (Video 1) or N-cadherin–coated beads (Video 2), and the GFP signal of cells associated with beads was acquired every 10 s for 300 ms/acquisition. Seventy-seven (Video 1) and 83 (Video 2) frames are shown at 1 frame per 1/6 s.

RESULTS

TI-VAMP Is Essential for Neurite Outgrowth

We have previously proposed that TI-VAMP mediates neurite outgrowth on the basis of the effect of overexpression of dominant-positive and -negative forms of the protein in PC12 cells and neurons (Martinez-Arca et al., 2000, 2001). In an independent approach, we sought to further analyze the role of TI-VAMP–mediated trafficking in neurite outgrowth. To this end, we designed siRNA (Elbashir et al., 2001) equivalent to the sequence of either rat or, as a control, dog TI-VAMP to silence the expression of the TI-VAMP protein in rat cells. Extracts of transfected cells were analyzed by Western blotting with antibodies against TI-VAMP, Syb, IgCAM L1, and transferrin receptor, and densitometric analysis of the corresponding signals was performed (Figure 1B). In siRNAr-transfected cells, total TI-VAMP expression was reduced to 30% (average more than three independent experiments) of that of siRNAd-transfected cells. No difference in the expression level of L1, transferrin receptor, and Syb was observed. To analyze the effect of silencing TI-VAMP expression on neurite outgrowth, we transfected PC12 cells with siRNAr or siRNAd and induced differentiation of PC12 cells by treatment with staurosporine for 24 h. To clearly identify transfected cells, we cotransfected small amounts of enhanced green fluorescent protein (EGFP) plasmid DNA with the siRNAs. By immunofluorescence, we found that the siRNAr-transfected GFP-positive cells were virtually devoid of TI-VAMP immunoreactivity, whereas no effect on TI-VAMP expression was seen in siRNAd-transfected cells
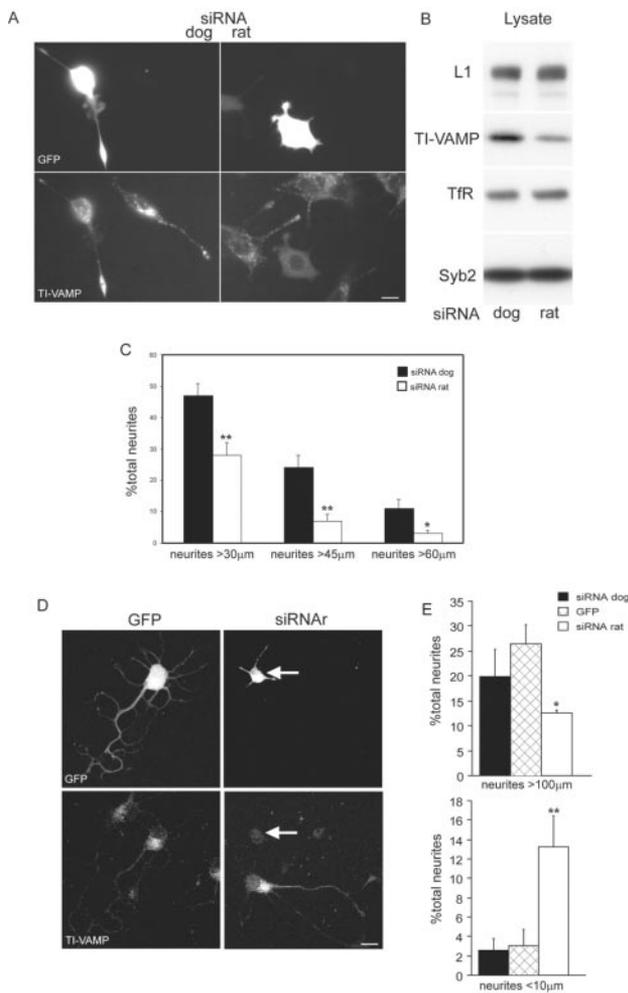
Figure 1. Silencing of TI-VAMP expression impairs neurite out-growth in PC12 cells and neurons. (A) PC12 cells were transfected with siRNAr or siRNAd combined with an expression plasmid encoding GFP. After 72 h, differentiation was induced by treatment with staurosporine for 24 h. SiRNAr silenced the expression of TI-VAMP and inhibited neurite outgrowth (GFP-positive cell, right), whereas siRNAd had no effect (GFP-positive cell, left) (bar, 5 μm). (B) Lysates of cells corresponding to A were analyzed by Western blotting for the expression levels of TI-VAMP, L1, transferrin receptor (TfR), and Syb 2. (C) The neurite length of GFP-positive cells transfected with siRNAr or siRNAd was quantified. Bars represent the percentage of the total number of neurites >30, 45, and 60 μm from two independent experiments (*p < 0.05; **p < 0.01). (D) TI-VAMP expression in hippocampal neurons was silenced by transfecting with siRNA and small amounts of EGFP vector. Three days after plating, TI-VAMP expression in EGFP-positive cells was assessed by immunofluorescence with mAb 158.2. As in PC12 cells, siRNAr decreased expression levels of TI-VAMP and inhibited neurite outgrowth (GFP-positive cell, right) compared with control cells (GFP-positive cell, left) (bar, 10 μm). (E) Quantification of axon lengths in neurons cotransfected with siRNAd or siRNAr and EGFP or transfected with EGFP alone is shown. Bars represent the percentage of total axons >100 μm (top) or <10 μm (bottom) from three independent experiments (*p < 0.02 with respect to GFP control; **p < 0.01 with respect to siRNAd control).

(Figure 1A). Silencing TI-VAMP expression led to a 25% reduction in the average neurite length in GFP-positive, siRNAr-tranfected cells compared with GFP-positive,

siRNAd-transfected cells (Figure 1A). The effect of reduced TI-VAMP expression on neurite length was particularly pronounced when the number of neurites >30, 45, or 60 μm was compared with control cells (Figure 1C). We then carried out similar experiments in immature neurons in primary culture from E18 rat hippocampi. We found that impaired expression of TI-VAMP in neurons leads to an inhibition of axonal outgrowth (Figure 1D). As with PC12 cells, a strong inhibition of neurite outgrowth by TI-VAMP silencing was observed when the number of neurites <10 μm or >100 μm of neurons transfected with GFP and siRNAr was compared with that of neurons transfected with GFP plus siRNAd or GFP alone (Figure 1E). Thus, TI-VAMP expression in PC12 cells and neurons in culture is necessary for efficient neurite outgrowth.

TI-VAMP Forms Complexes with SNAP25, Syntaxin 1, Syntaxin 7, and Vti1b In Vivo

The latter results demonstrate that the membrane-trafficking pathway mediated by TI-VAMP is essential for neuronal differentiation, yet the nature of this pathway is not clear. A function of TI-VAMP in endocytosis has been suggested by several studies in nonneuronal mammalian cells (Advani *et al.*, 1999; Wade *et al.*, 2001) as well as in *Dictyostelium discoideum* (Bogdanovic *et al.*, 2002). We have previously shown that TI-VAMP recycles to the plasma membrane in neuronal cells and forms SNARE complexes with the plasma membrane t-SNARE SNAP25 (Martinez-Arca *et al.*, 2000). To identify the target membranes of TI-VAMP–containing vesicles in neuronal cells, we sought to identify the full catalog of cognate t-SNARE partners of TI-VAMP. To this end, we searched for t-SNAREs that would coimmunoprecipitate with TI-VAMP from a Triton X-100 extract of rat brain. TI-VAMP was specifically immunoprecipitated by the mAb 158.2 but not by control IgGs. We also recovered the plasma membrane t-SNAREs SNAP25 and Stx 1, and the endosomal t-SNAREs Stx 7 and Vti1b with the TI-VAMP immunobeads (Figure 2A). Importantly, we did not observe complex formation with another endosomal t-SNARE, syntaxin 13. The recombinant forms of syntaxin 13 and TI-VAMP are able to interact in vitro (Yang *et al.*, 1999); thus, the absence of syntaxin 13 in our assay suggests that the complexes we isolated were not formed during the process of detergent solubilization of the tissue. Furthermore, when we determined the subcellular distribution of TI-VAMP and Stx 7 in primary corticostriatal cultures grown for one division, extensive colocalization of both proteins on vesicular structures in the cell body and along the growing neurites was observed (Figure 2B). These results show that TI-VAMP forms cognate SNARE complexes with the plasma membrane syntaxins SNAP 25 and Stx 1 and the endosomal SNAREs Stx 7 and Vti1b in the adult rat brain and suggest that TI-VAMP mediates a recycling pathway that connects the plasma membrane with an endosomal Stx 7-containing compartment in neurons.

The IgCAM L1 Is a Cargo Molecule of the TI-VAMP Compartment

To further understand the role of TI-VAMP–mediated trafficking in the differentiation of neuronal cells, we sought to identify cargo molecules of the TI-VAMP compartment. Candidate molecules included CAMs such as integrins, cadherins, and CAMs of the IgCAMs, owing to their essential role in brain development. The IgCAM L1 is particularly interesting in this context because it actively recycles with the neuronal plasma membrane during axonal outgrowth
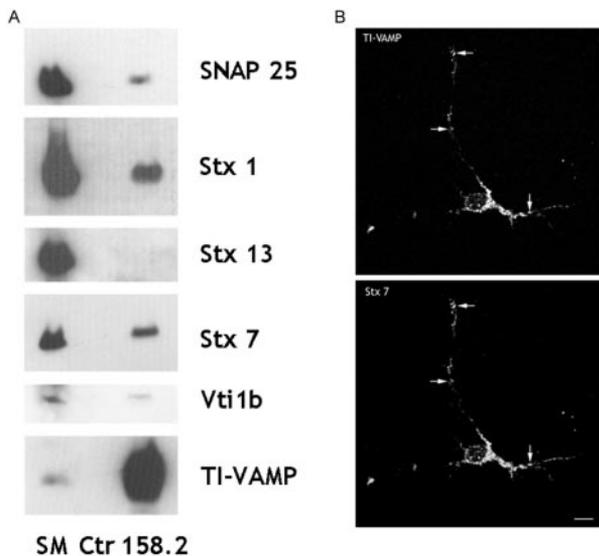
Figure 2. TI-VAMP forms SNARE complexes with plasma membrane and endosomal t-SNAREs and colocalizes with Stx 7. (A) SNARE complex formation of TI-VAMP in rat brain. The Triton X-100–soluble fraction of rat brain was incubated with mAb 158.2 or control IgGs (Ctr) covalently coupled to protein G-Sepharose. An aliquot of the starting material (SM) and material bound to immunobeads was analyzed by Western blotting with antibodies to TI-VAMP, Vti1b, Stx7, Stx 13, Stx1, and SNAP25. (B) Localization of TI-VAMP and syntaxin 7 in cortical/striatal neurons in culture. E16 rat cortical-striatal neurons were grown for 1 d in vitro, labeled for TI-VAMP and syntaxin 7, and analyzed by confocal microscopy. Vesicular structures positive for TI-VAMP and Stx 7 are indicated by arrows (bar, 5 μm).

Figure 3. TI-VAMP and L1 are coexpressed in growing axonal tracts in the developing rat brain. Expression of L1 and TI-VAMP in the developing brain. E15 and E19 embryos were serially sectioned in the sagittal plane and labeled for TI-VAMP and L1 (right). In all four examples shown there is a high degree of colocalization. (A) Olfactory nerve branching out in the olfactory epithelium. (B and C) Trigeminal ganglion and nerve root. In B, the trigeminal nerve ganglion contains TI-VAMP–labeled neurons. Their labeled axons are seen to converge toward the brainstem, and in C, trigeminal nerve branches fan out toward the facial vibrissae (left). (D) In the forebrain, TI-VAMP–labeled axon tracts are observed that correspond to corticofugal pathways and to cortical afferent pathways (bar, 100 μm).

(Kamiguchi and Lemmon, 2000a). To investigate the possible relationship between L1 trafficking and TI-VAMP, we analyzed the expression of both proteins in the developing rat brain by confocal microscopy on embryonic brain cross sections. During embryonic life, corresponding to the phases of active axon outgrowth, TI-VAMP labels a large number of axons in cranial nerves such as the olfactory nerve, the trigeminal nerve (Figure 3, A–C), and major central axon tracts, such as the thalamocortical tract (Figure 3D) and the medial forebrain bundle (our unpublished observations). In all these locations, TI-VAMP–labeled axons coexpressed L1. These observations suggest that TI-VAMP could indeed play a role in L1 function during active axonal outgrowth.

We then analyzed the expression pattern of L1 and TI-VAMP at a subcellular level in PC12 cells and hippocampal neurons by using confocal microscopy. In undifferentiated PC12 cells grown at low density, we found that L1 expression was not restricted to the plasma membrane but that a considerable intracellular pool of L1 could be detected. This pool coincided largely with TI-VAMP–positive vesicular structures (Figure 4A, arrows). When L1 is used as a substrate, axonal outgrowth is greatly stimulated in several neuronal cell types, (Lemmon et al., 1989) (Figure S1), owing to homophilic interactions between L1 on the neurons and on the substrate (Lemmon et al., 1989; Dahme et al., 1997). Therefore, it was of interest to analyze the subcellular localization of L1 in hippocampal neurons grown on L1, and thus engaged in homophilic adhesion, and compare it with the localization of TI-VAMP. In the growth cone of the growing axon as well as in the cell body, L1 was expressed on the plasma membrane and, in addition, an intracellular
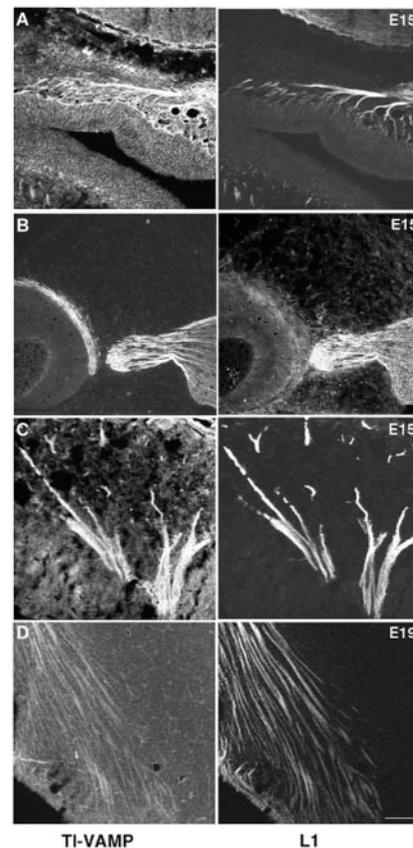
pool of L1 could be observed (Figure 4, B and C). Importantly, we found considerable colocalization between the intracellular pool of L1 and TI-VAMP at the tip of the growing axon (Figure 4B) and in cell bodies (Figure 4C). Occasionally, we observed a striking accumulation of TI-VAMP and L1 immunoreactivity at sites of cell-cell contact. L1 seemed to be in part vesicular at these sites, which was not the case in varicosities where L1 was at the plasma membrane (Figure 4C).

We then partially purified the TI-VAMP membrane compartment by subcellular fractionation of PC12 cells and adult rat brain. Velocity gradient analysis of PC12 cells showed that TI-VAMP and L1 immunoreactivity were enriched in the top four fractions of the gradient (Figure 5A, velocity gradient). This pool of membranes did not contain significant amounts of Na/K-ATPase, a plasma membrane protein that does not recycle with endosomal compartments (Le et al., 1999). When these four fractions were pooled and separated by subsequent density gradient centrifugation, we found cofractionation of L1 and TI-VAMP with membranes
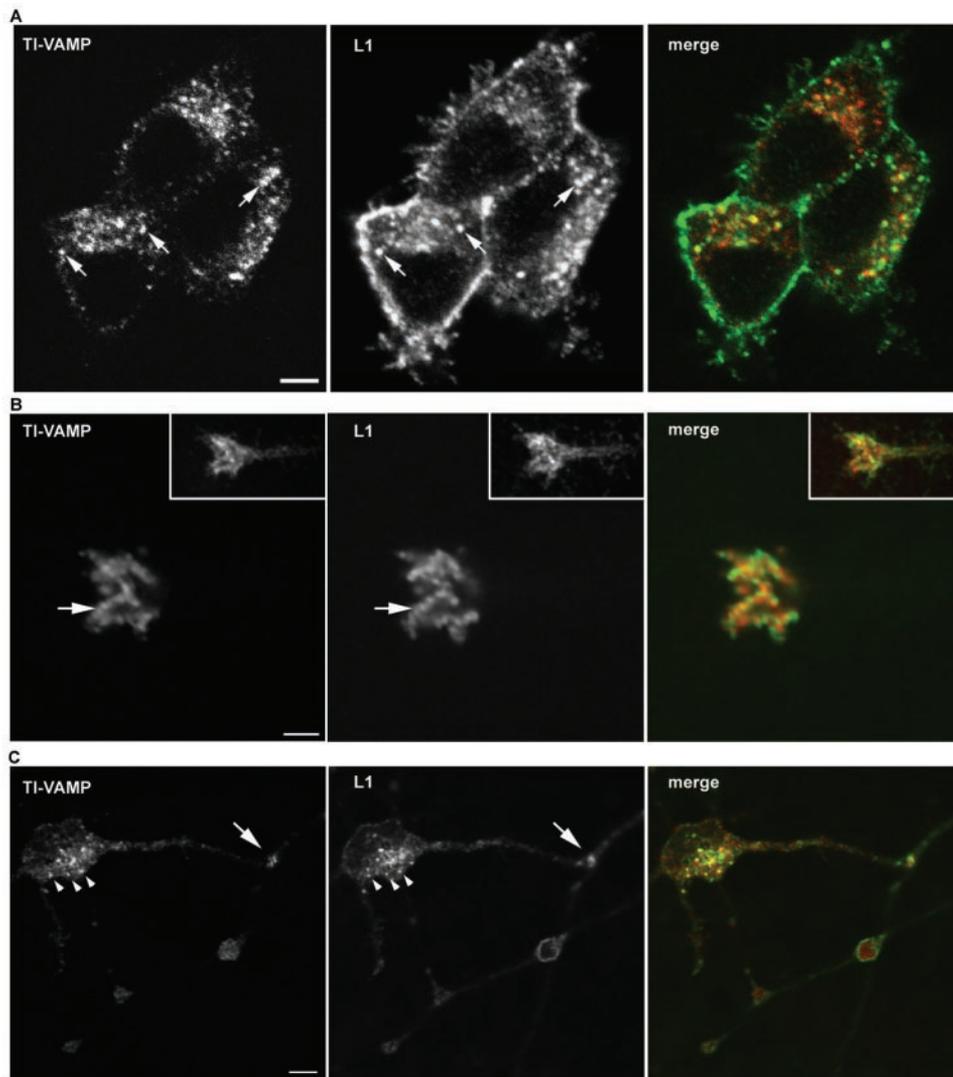
Figure 4. TI-VAMP and L1 colocalize in neurons grown in culture. (A) Localization of TI-VAMP and L1 in PC12 cells. PC12 cells were grown at low density in the absence of NGF and processed for immunofluorescence analysis by confocal microscopy. A considerable pool of L1 immunoreactivity (green) is located on intracellular structures, which largely coincides with TI-VAMP expression (red), as indicated by arrows (bar, 4 μm). (B and C) Localization of TI-VAMP and L1 in neurons grown on L1. Hippocampal neurons were grown for 1 d in vitro on L1 and labeled for TI-VAMP and L1. (B) The confocal sections were taken from the apical part of the growth cone shown in the inset. The arrow points to a row of vesicular structures positive for TI-VAMP (red) and L1 (green); most of L1 (green) at the tip of the growth cone accumulates in clusters at the plasma membrane (bar, 3.5 μm). (C) Two contacting neurons are shown. The arrowheads point at vesicular structures in the cell body of a neuron, which are positive for L1 and TI-VAMP expression. Note also the accumulation of L1 and TI-VAMP immunoreactivity where a neurite extending from the cell body is forming a contact with a passing axon (arrow) (bar, 7 μm).

of similar density, which were clearly different from plasma membrane (Figure 5A, equilibrium gradient; and Figure S2). We then applied the same approach to fractionate adult rat brain. The supernatant of a low-speed centrifugation of rat brain homogenate (S1) was separated by medium-speed centrifugation to yield the supernatant S2 and the pellet P2. An antibody directed against the extracellular domain of L1 detected three major reactive species of 220, 140, and 80 kDa (Figure 5B). These three species correspond to full-length L1 (L1–220) and the two cleavage products resulting from a specific proteolysis within the third fibronectin type III domain of L1, yielding extracellular L1–140 and membrane-bound L1–80 (Liljelund *et al.*, 1994; Silletti *et al.*, 2000). Whereas Na/K-ATPase and L1–80 were heavily enriched in

fraction P2, a small pool of L1–220 and L1–140 immunoreactivity was detectable in S2. TI-VAMP showed an equal distribution between S2 and P2. Because S2 was poor in plasma membrane proteins, we decided to further analyze the membrane population of S2 by velocity and equilibrium gradient centrifugation. As in PC12 cells, velocity gradient centrifugation of S2 led to an enrichment of TI-VAMP–positive membranes in the upper fractions of the gradient (Figure 5B, velocity gradient), which also contained L1–220, whereas plasma membrane peaked in fraction 3 as seen by L1–80 staining. Subsequent equilibrium gradient centrifugation of these first two fractions clearly separated plasma membrane from TI-VAMP–positive membranes, as shown by the peak of expression of L1–80 and Na/K-ATPase in
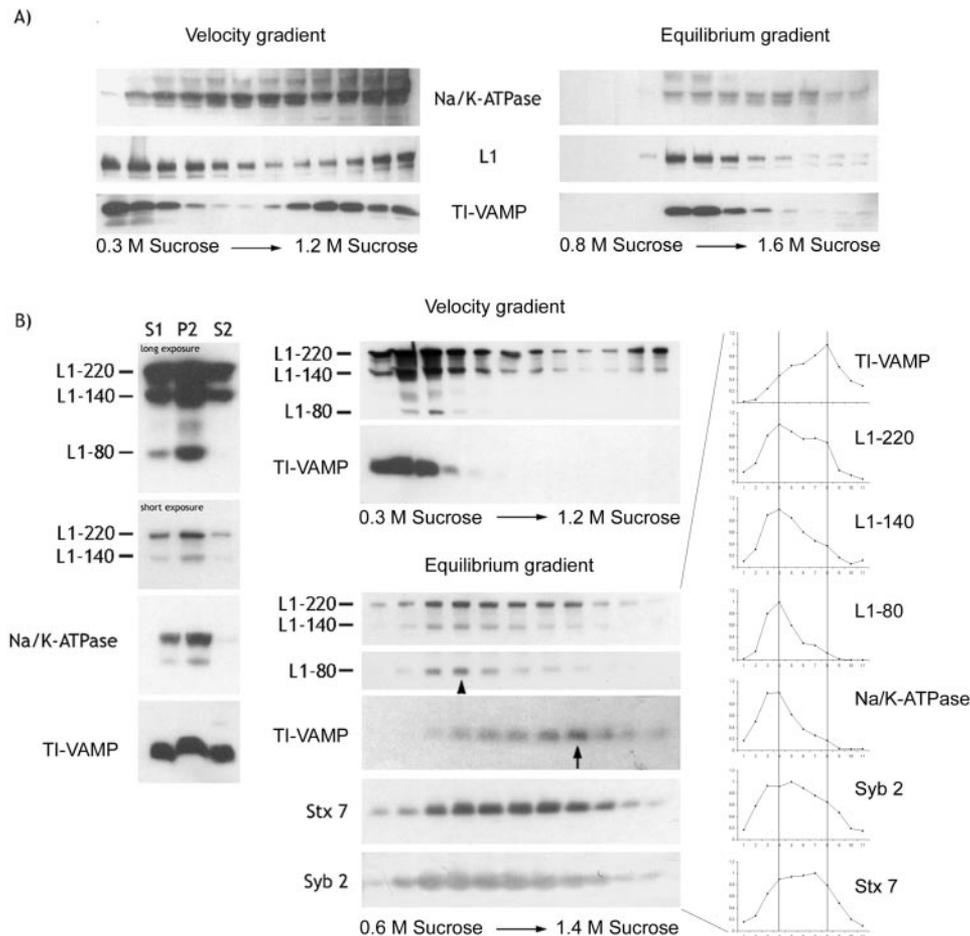
Figure 5. An intracellular pool of L1 cofractionates with TI-VAMP–positive membranes in PC12 cells and adult rat brain. (A) Fractionation of membranes from PC12 cells positive for TI-VAMP and L1 in velocity and equilibrium gradients. PC12 cells were homogenized and membranes were separated on a continuous sucrose gradient by velocity gradient centrifugation. The first four fractions of the gradient were pooled and subjected to equilibrium gradient centrifugation on a continuous sucrose gradient. Equal volumes of each fraction were analyzed by Western blotting with antibodies to TI-VAMP, L1, and Na/K-ATPase. (B) Fractionation of membranes from rat brain positive for TI-VAMP and L1 in velocity and equilibrium gradients. Rat brain was homogenized and the supernatant of a low-speed centrifugation (S1) was subjected to a medium-speed centrifugation to yield a pellet, P2, and a supernatant, S2. Equal amounts of protein were analyzed by Western blotting for TI-VAMP, L1, and Na/K-ATPase expression. An aliquot of S2 was loaded on top of a continuous sucrose gradient, and membranes were separated by velocity gradient centrifugation. Fractions were collected and Western blot analysis of equal volumes of each fraction was performed with antibodies to TI-VAMP, L1, and Na/K-ATPase. The first two fractions were pooled and centrifuged to equilibrium. Analysis was performed as described above with antibodies to TI-VAMP, L1, Na/K-ATPase, Syb 2, and syntaxin 7. The corresponding signals were quantified by densitometry, the peak signal was defined as 1, and the resulting graphs are shown adjacent to the Western blot.

fractions 3 and 4 (arrowhead and quantification) compared with the peak of TI-VAMP expression in fraction 9 (arrow) (Figure 5B, equilibrium gradient and quantification). Interestingly, L1–220 immunoreactivity was found in a broad distribution from light membranes, presumably corresponding to L1 associated with plasma membrane, to denser membranes where it coincided with TI-VAMP (Figure 5B, equilibrium gradient and quantification). L1–140 showed a distribution indicating a main association with the plasma membrane, but in addition a partial association with intracellular membranes (Figure 5B, equilibrium gradient and quantification). The pool of membranes positive for L1 and TI-VAMP expression was different from synaptic vesicles because they were found at lower densities, as seen by expression of Syb 2. Stx 7 showed a broad distribution throughout the gradient, which was very similar to L1–220

and TI-VAMP in fractions 7–11, in agreement with the data in Figure 1 showing complex formation and colocalization of TI-VAMP and Stx 7 (Figure 5B, equilibrium gradient and quantification). Previous studies (Kamiguchi and Lemmon, 2000b; Kamiguchi and Yoshihara, 2001) suggest that the intracellular pool of L1 that we observed by immunofluorescence analysis (Figure 4) and subcellular fractionation (Figure 5) may correspond to molecules that recycle to the plasma membrane. To test this hypothesis, we incubated living PC12 cells with Fab fragments directed against L1. We detected a punctate labeling for L1-specific Fab fragments along the neurites and within the cell bodies (Figure 6A), demonstrating that plasma membrane L1 was endocytosed in NGF-differentiated PC12 cells, as described for neurons from dorsal root ganglia (Kamiguchi and Lemmon, 2000b; Kamiguchi and Yoshihara, 2001). The punctate staining of
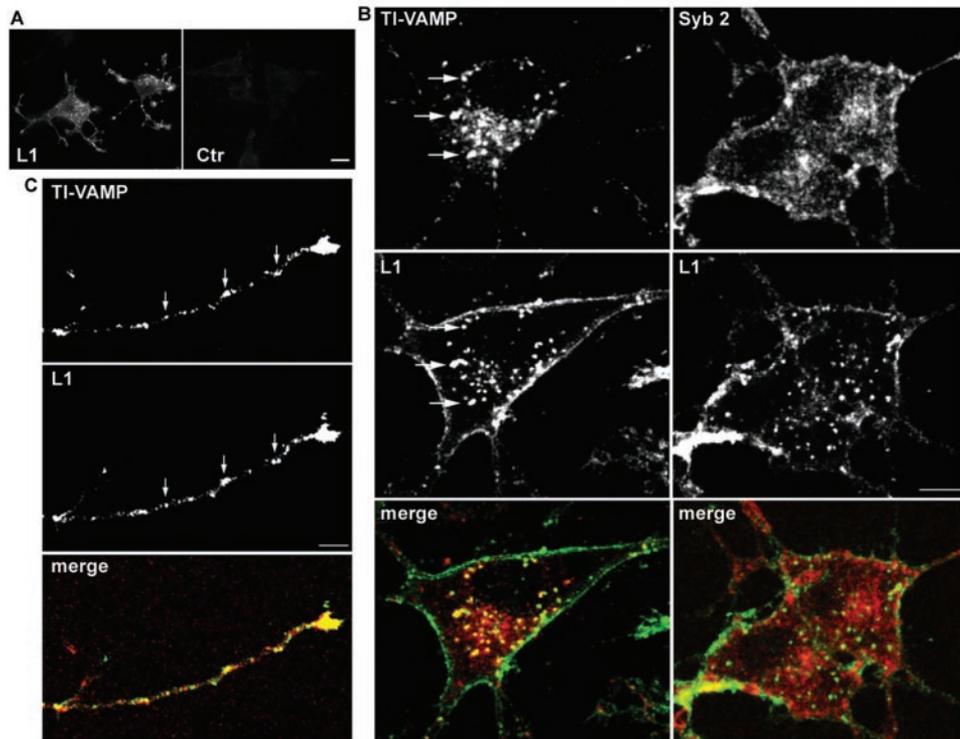
Figure 6. Endocytosed L1 reaches the TI-VAMP compartment but is absent from the Syb 2-compartment. (A) L1 is endocytosed in NGF-differentiated PC12-cells. PC12 cells were grown in the presence of NGF for 48 h. Cells were incubated with L1-specific Fab fragments or control IgGs. The cells were "acid stripped" and processed for immunofluorescence analysis (bar, 8 μm). (B) L1 is taken up into the TI-VAMP compartment but not into the Syb 2 compartment. NGF-differentiated PC12 cells were incubated with L1-specific Fab fragments (green) as described above and labeled for TI-VAMP (red) or Syb 2 (red). Arrows highlight intracellular structures positive for TI-VAMP and endocytosed L1-specific Fab fragments (green) (bar, 5 μm). (C) L1 is taken up into the TI-VAMP compartment in neurons in culture. Cortical-striatal neurons grown on collagen were incubated with Fab-fragments directed against L1. After removal of the Fab fragments, the neurons were further incubated at 37°C, fixed, and labeled for TI-VAMP (red) and endocytosed L1 (green). Arrows point at structures in the growing axon positive for TI-VAMP and endocytosed anti-L1 Fab fragments (bar, 3 μm).

L1-specific Fab fragments did not correspond to unspecific fluid phase uptake of the antibody because we could not detect uptake of control immunoglobulins used at the same concentration (Figure 6A). We then asked whether endocytosed L1 would reach, and be restricted to, TI-VAMP's compartment. We incubated NGF-differentiated PC12 cells with L1-specific Fab fragments and costained for either TI-VAMP or Syb 2 as a marker for the well-characterized compartment of regulated exocytosis in PC12 cells. Analysis by confocal microscopy, shown in Figure 6B, demonstrated that endocytosed L1 labeled with L1-specific Fab fragments colocalized to a great extent with TI-VAMP in punctate structures scattered around the perinuclear region (arrows). In contrast, no colocalization of endocytosed L1 was observed with the Syb 2-positive compartment in PC12 cells (Figure 6B). We extended our analysis of the endocytic trafficking of L1 and TI-VAMP to neurons grown in culture. Plasma membrane L1 underwent endocytosis in neurons differentiating in primary culture as confocal microscopy revealed a punctate labeling for L1 Fab fragments along the axon (Figure 6C). These intracellular structures of endocytosed L1 coincided with structures positive for TI-VAMP expression (marked by arrows). Together, these results show that L1 is specifically endocytosed into the TI-VAMP–containing compartment. This prompted us to investigate the function of TI-VAMP–mediated trafficking in L1-mediated adhesion.

TI-VAMP Is Required for L1-Mediated Adhesion

The biological function of L1 as a homophilic adhesion molecule can be mimicked by presenting recombinant L1 on a planar substrate (Figure S1) or coated on beads (Kamiguchi and Yoshihara, 2001; Yip and Siu, 2001). This approach allows the analysis of L1-specific adhesive contacts isolated from the complex situation that occurs when two cells form contacts. Therefore, we adopted a bead assay that was successfully used to analyze the functional consequences of N-cadherin–mediated contact formation (Lambert *et al.*, 2000). Stable contact formation of L1 beads with PC12 cells was dependent on the presence of recombinant L1 on the beads, because no beads were found associated with PC12 cells when L1 was omitted during the coating procedure (our unpublished observations). For insight into the role of TI-VAMP in L1-mediated adhesion, we silenced TI-VAMP expression with siRNA in PC12 cells and incubated the cells with beads coated with the extracellular domain of L1. We used N-cadherin–coated beads as a control, because it has been suggested that the function of N-cadherin is independent of intracellular trafficking in neurons (Kamiguchi and Yoshihara, 2001). We found a reduction of 50% in the number of L1 beads associated with cells treated with siRNAr compared with cells treated with siRNAd (Figure 7, A and B). In contrast, we did not find any effect on the amount of
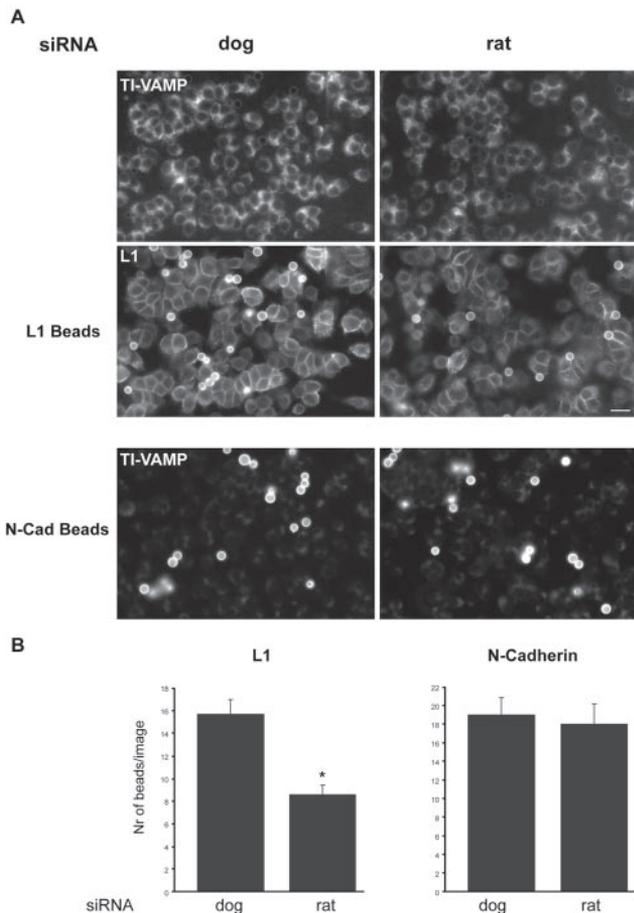
Figure 7. TI-VAMP–mediated intracellular trafficking is essential for L1-dependent adhesive contacts. (A) Binding of L1-coated beads to PC12 cells is inhibited by silenced TI-VAMP expression. PC12 cells were treated with siRNA dog or rat and incubated with beads coated with L1-Fc or N-cadherin-Fc chimeras. Immunofluorescence was performed with mAb 158.2 and polyclonal L1-antibody. Note that N-cadherin beads are labeled by Cy3-coupled anti-mouse secondary antibody due to the presence of the mouse Fc fragment in N-cadherin chimera (bar, 20 μm). (B) Binding of L1 and N-cadherin–coated beads to siRNA-treated PC12 cells was quantified by counting the number of beads per image (*p < 0.01).

N-cadherin beads attached to cells treated with either siRNA rat or dog (Figure 7, A and B). We performed similar experiments to analyze the effect of inhibiting TI-VAMP–dependent trafficking on the surface expression of L1. PC12 cells were treated with siRNAr/d and incubated at 4°C with the anti-L1 antibody before fixation. Quantification of L1-associated immunoreactivity revealed that L1 surface expression was reduced to ~80% in siRNAr-treated cells compared with control cells (n = 4, p < 0.02) (compare also Figure 7A, L1 panels). This result demonstrates that TI-VAMP–mediated trafficking is essential for surface expression of L1 and the stability of L1-dependent adhesive binding events and thus for the proper function of L1 at the plasma membrane. This result also shows that N-cadherin–mediated adhesive junctions are independent of TI-VAMP trafficking and suggests that the functions of L1 and N-cadherin at the plasma membrane of PC12 cells are regulated in different ways.

L1 Controls TI-VAMP–Mediated Trafficking

The latter results indicate that L1 function at the plasma membrane is controlled by the TI-VAMP–trafficking pathway. In turn, it is known that activation of L1 at the plasma membrane induces a signaling cascade important for L1 function (Schaefer et al., 1999; Schmid et al., 2000). Therefore, it was of interest to analyze whether local activation of plasma membrane L1 due to L1 bead contacts would have an effect on TI-VAMP trafficking. By confocal microscopy, we analyzed the subcellular localization of TI-VAMP and L1 in PC12 cells incubated with L1-coated beads. As shown in Figure 8A, L1-dependent contact formation between cell and bead led to a striking accumulation of plasma membrane L1 at sites of contact, indicating homophilic binding between L1 bead and L1 at the cell surface. Furthermore, vesicles positive for both L1 and TI-VAMP could often be observed in proximity to the contact site (Figure 8A, arrows). To analyze the dynamics of the recruitment of TI-VAMP vesicles to L1-mediated contact sites, we expressed GFP-TI-VAMP in PC12 cells and incubated the cells with L1- or N-cadherin–coated beads. Time-lapse videomicroscopy revealed a recruitment of GFP-TI-VAMP to the L1 bead to cell contact, which was stable for the entire time of recording (20 min) (Figure 8B, arrow; Video 1). At the same time, GFP-TI-VAMP vesicles more distant to the bead-cell contact showed a dynamic localization with clusters of vesicles, appearing and disappearing in several domains of the cytoplasm (Figure 8, arrowhead; Video 1). We did not observe any accumulation of TI-VAMP-GFP close to sites of N-cadherin bead-cell contact (Figure 8; Video 2), indicating that N-cadherin–dependent outside-in signaling events do not influence TI-VAMP trafficking. Together, these results suggest that L1-mediated adhesion promotes a local accumulation of TI-VAMP–containing vesicles at sites of L1 bead-to-cell contact.

The accumulation of TI-VAMP–containing vesicles at sites of L1 bead-cell contact was even more striking when hippocampal neurons were incubated with L1-coated beads. As shown in Figure 9A, L1-coated beads bound to axonal growth cones induced a strong accumulation of TI-VAMP immunoreactivity at sites of bead cell contact as seen by the appearance of bead-shaped structures strongly labeled for TI-VAMP, especially in the apical planes of the confocal sections shown (i.e., where the bead surface is surrounded by the growth cone membrane). The accumulation of TI-VAMP at sites of bead-growth cone contact was a very robust phenomenon that could be observed in six of eight examples, when images were taken based on the L1 signal (i.e., in blind for associated TI-VAMP immunoreactivity) (Figure S3). Like with PC12 cells, the binding of beads to neurons was strictly dependent on the presence of the L1-Fc fragment (our unpublished observations). We then compared the behavior of the TI-VAMP compartment to the Syb 2 compartment when an L1-coated bead is contacting a growth cone. As seen in Figure 9B, TI-VAMP immunoreactivity was particularly enriched in the apical plane of the confocal sections of the growth cone shown, where a bead-shaped structure like in Figure 9A was observed. In contrast, Syb 2 reactivity decreased from the basal to the apical plane of the growth cone and no formation of a bead-like structure was seen. We quantified the average pixel intensity in the basal and apical region of TI-VAMP and Syb 2 immunoreactivity in eight growth cones in contact with a bead
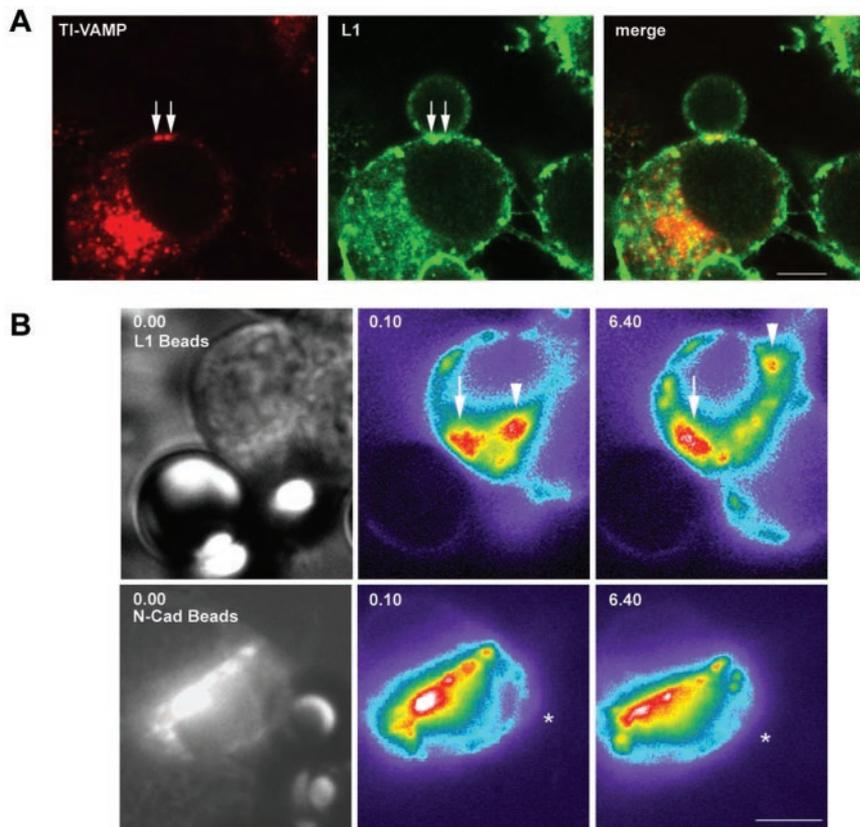
Figure 8. L1-dependent adhesive contacts induce clustering of TI-VAMP–positive vesicles at sites of contact in PC12 cells. (A) TI-VAMP vesicles accumulate at sites of L1-bead contact. PC12 cells were incubated with L1-coated beads, processed for immunofluorescence with mAb 158.2 and polyclonal antibody to L1, and analyzed by confocal microscopy. Arrows point at TI-VAMP–positive intracellular structures clustered around the bead cell contact, which are also positive for L1 (bar, 5 μm). (B) L1-beads induce stable clusters of TI-VAMP-GFP. PC12 cells were transfected with TI-VAMP-GFP and incubated with L1-coated beads (top) or N-cadherin–coated beads (bottom). Dynamics of TI-VAMP-GFP were observed by time-lapse videomicroscopy. Shown are snapshots taken with phase contrast (left) and with GFP-filters (middle and right, shown in false color to highlight concentration of TI-VAMP-GFP signal). A stable accumulation of TI-VAMP-GFP close to the site of L1-bead to cell contact could be observed during the recording time (indicated by arrow). A second pool of TI-VAMP-GFP signal indicated by an arrowhead showed a dynamic behavior. N-Cadherin–coated beads did not show any influence on the dynamic behavior of TI-VAMP-GFP (position of N-cadherin bead in false colored images is indicated with asterisk) (bar, 6 μm). See supplemental videos at www.molbiolcel-l.org .Video 1, dynamics of TI-VAMP-GFP in PC12 cells in contact with a L1-coated bead. PC12 cells were transfected with TI-VAMP-GFP and incubated with L1-coated beads. TI-VAMP-GFP signal was recorded over a time frame of 20 min with exposures of 300 ms every 10 s. Shown is an extract of 77 frames at a display rate of 1 frame per 1/6 s. The starting frame of the video shows the bead contacting the recorded cell in phase contrast. Video 2, dynamics of TI-VAMP-GFP in PC12 cells in contact with a N-cadherin–coated bead. PC12 cells were TI-VAMP-GFP transfected and incubated with N-cadherin–coated beads. Acquisition of GFP signal was performed as above. Shown is an extract of 83 frames at the same display rate as in Video 1. The starting frame of the video shows the bead contacting the recorded cell in phase contrast.

(see MATERIALS AND METHODS for details). In the case of Syb 2, the ratio between apical to basal average pixel intensity was found to be 0.4 ± 0.06, indicating a sharp decrease in fluorescence intensity from the basal to the apical plane. In contrast, using the same parameters to analyze TI-VAMP distribution in the same growth cones, we found a ratio close to 1 (0.9 ± 0.085). The difference between the apical-to-basal ratio of Syb 2 and TI-VAMP was statistically significant ($p = 0.01$; Mann-Whitney nonparametric test). Thus, L1-coated beads contacting an axonal growth cone induced a strong and specific accumulation of the TI-VAMP compartment in proximity to the cell bead contact compared with the Syb 2 compartment.

DISCUSSION

In this study, we demonstrate that TI-VAMP expression is necessary for neurite outgrowth and L1-mediated adhesion. Furthermore, L1-mediated adhesion controls TI-VAMP–mediated trafficking. This model is based on the following evidence presented herein: 1) impaired expression of TI-VAMP by RNAi strongly inhibits neurite outgrowth in PC12 cells and hippocampal neurons in culture; 2) TI-VAMP colocalizes with L1 in situ in the developing brain, in PC12 cells and neurons, and endocytosed L1 is localized to the TI-VAMP compartment; 3) impaired TI-VAMP expression

affects surface expression of L1 and reduces the binding of L1-coated beads to PC12 cells; and 4) L1-dependent adhesive contacts induce local clustering of TI-VAMP but not Syb 2 vesicles and control the dynamics of TI-VAMP at sites of contact, suggesting that L1-mediated adhesion controls the anchoring of TI-VAMP–containing vesicles. Therefore, this report demonstrates a cross talk between TI-VAMP–dependent trafficking and L1-mediated adhesion and L1-induced signaling and TI-VAMP dynamics.

TI-VAMP Is Required for Neurite Outgrowth

A strong decrease of TI-VAMP expression was achieved by RNA interference in PC12 cells and hippocampal neurons in primary culture. This resulted in the inhibition of neurite outgrowth, thus providing genetic evidence that TI-VAMP is essential for neurite outgrowth. This result confirms and extends our previous studies (Martinez-Arca *et al.*, 2000, 2001) in which we had used dominant-positive and -negative forms of TI-VAMP to suggest that this membrane-trafficking pathway is important for axonal and dendritic outgrowth. Our present finding that TI-VAMP–mediated trafficking is required for normal neurite outgrowth demonstrates that membrane trafficking plays an important role in this process. Also, this underlines the high degree of compartmentalization of neuronal cells and the specificity of v-SNAREs in mediating distinct membrane-trafficking path-
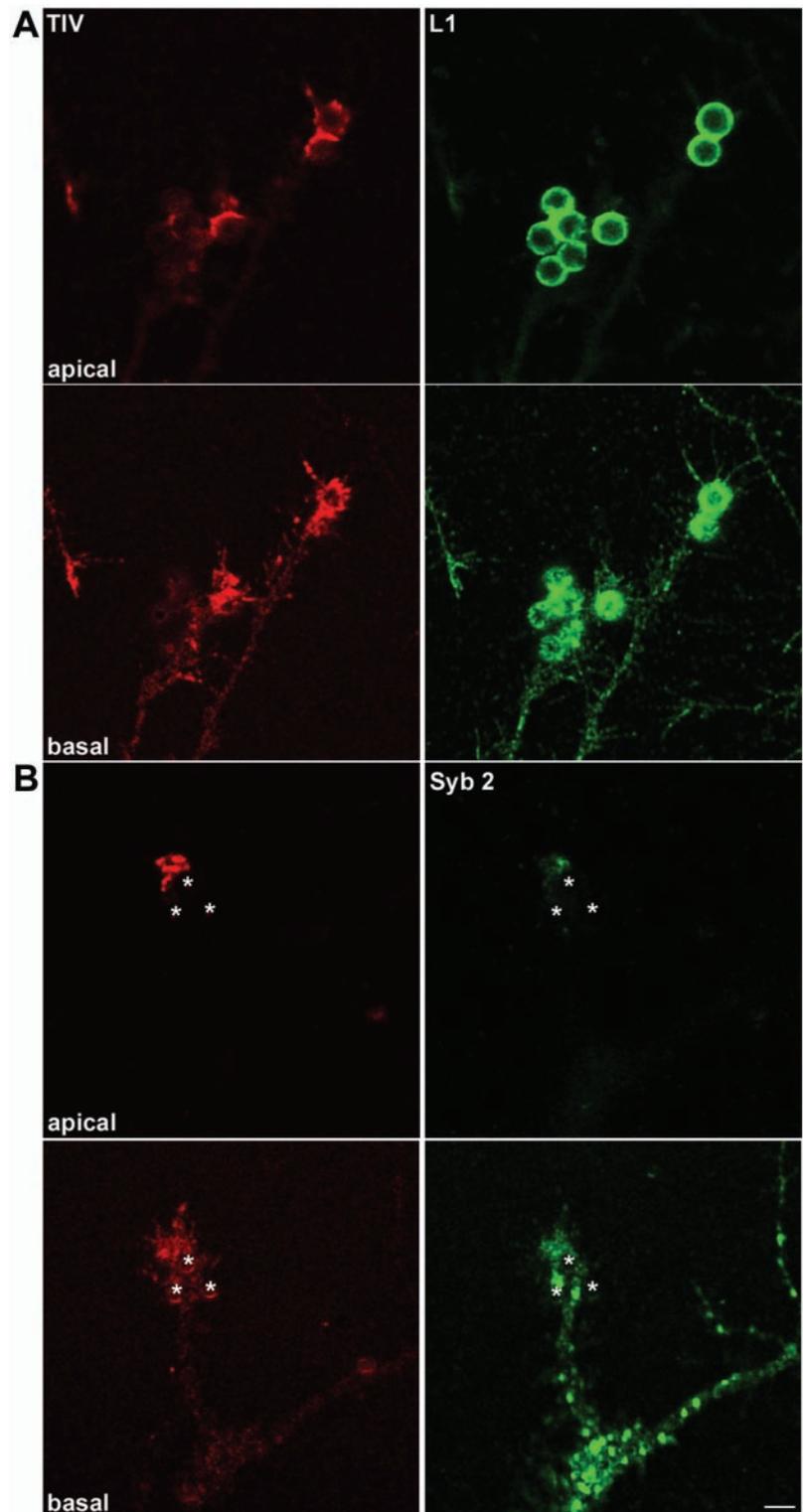
Figure 9. L1-dependent adhesive contacts induce clustering of TI-VAMP but not Syb 2-positive vesicles in neuronal growth cones. (A) Accumulation of TI-VAMP at bead/growth cone junctions. Hippocampal neurons grown for 3 d in vitro were incubated with L1-coated beads and processed for confocal microscopy analysis with mAb 158.2 (red) and polyclonal antibody to L1 (green). A basal and an apical section of the same region are shown. Note the formation of bead shaped, TI-VAMP–positive structures in the growth cones. (B) Comparison between TI-VAMP and Syb 2 compartment in a growth cone contacting a bead. Hippocampal neurons were incubated with L1 beads and processed for immunofluorescence with mAb 158.2 and polyclonal antibody to Syb 2. A basal and an apical section of the same region are shown and bead positions are indicated by asterisks. Note the strong TI-VAMP immunoreactivity in the apical confocal section as compared with the basal section (bar, 4 μm).

ways. Similar conclusions were drawn from the analysis of another neuronal v-SNARE Syb 2, which was shown to be essential for neurotransmitter release, but, in contrast to TI-VAMP, dispensable for neuronal differentiation (Osen-Sand *et al.*, 1996). In vivo confirmation of these observations was obtained by the analysis of mice mutant for Syb 2,

which show an almost complete block in neurotransmitter release, but apparently normal brain development (Schoch *et al.*, 2001). In contrast, whereas SNAP25 antisense oligonucleotides and botulinum neurotoxin A inhibited neurite outgrowth (Osen-Sand *et al.*, 1993, 1996), this finding was not confirmed in the knockout mice (Washbourne *et al.*, 2002).

However, neurons express several syntaxins and both SNAP23 and SNAP25 (Chen *et al.*, 1999), so it can be anticipated that only the genetic invalidation of several plasma membrane SNAREs (at least SNAP25 and SNAP23) will result in defects in the development of the brain. Future studies are required to unravel the exact composition of SNAREs and their regulators involved in the differentiation of neurons.

L1 Recycles in the TI-VAMP Compartment

We have previously shown that TI-VAMP defines a new tubulo-vesicular compartment particularly concentrated at the leading edge of growth cones in hippocampal neurons developing in vitro. We also showed that TI-VAMP does not colocalize with either markers of synaptic vesicles or with several markers of endocytic compartments, except CD63 (Coco *et al.*, 1999). Like other tetraspanins, CD63 has been implicated in integrin-mediated cell migration (Berditchevski, 2001). Studies on the function of TI-VAMP suggested an involvement of TI-VAMP in late endocytic pathways in nonneuronal mammalian cells (Advani *et al.*, 1999; Wade *et al.*, 2001) as well as in *D. discoideum*, where it was shown to participate in an endosomal SNARE complex composed of Stx 7 and 8 and vti1b (Bogdanovic *et al.*, 2002). In agreement with these findings, we show herein that internalized L1 reaches the TI-VAMP compartment in neuronal cells and that TI-VAMP forms a SNARE complex with syntaxin 7 and vti1b and colocalizes with the endosomal t-SNARE syntaxin 7. Yet, our data point to a function of TI-VAMP that is more likely to correspond to a recycling rather than a degradative pathway in neuronal cells. This is supported by the finding that TI-VAMP forms SNARE complexes with the plasma membrane SNAREs syntaxin 1 and SNAP25. Importantly, TI-VAMP controls the surface expression of L1, thus clearly indicating that TI-VAMP mediates an exocytic pathway in neuronal cells. The previous findings that TI-VAMP colocalizes with CD63 in PC12 cells (Coco *et al.*, 1999) and HeLa cells (Martinez-Arca *et al.*, 2003b) could suggest that TI-VAMP's compartment corresponds to a specialized recycling endosome to which L1 (L1–220 and possibly L1–140) would be targeted after internalization and from which it would then be recycled to the plasma membrane. The TI-VAMP compartment could be related to the recently identified enlargosome, a compartment involved in membrane repair whose exocytosis is tetanus neurotoxin-insensitive (Borgonovo *et al.*, 2002). It will be important to get a more complete picture of the cargo proteins targeted to the TI-VAMP compartment to further understand the nature and molecular composition of this compartment.

Functional Cross Talk between TI-VAMP and L1

Our finding that L1-dependent adhesion is impaired by reduced expression of TI-VAMP clearly points to an essential role of TI-VAMP–dependent trafficking in the function of L1 at the plasma membrane. Interestingly, neuronal L1 harbors an additional short exon that yields a tyrosine-based motif YRSLE. This motif mediates binding to the AP-2 adaptor complex and clathrin-dependent endocytosis and accelerates the recycling of neuronal L1 (Kamiguchi *et al.*, 1998) suggesting a role for intracellular trafficking in L1 function, especially in the course of neuronal development. In analogy to migrating cells, it was suggested that L1 trafficking in the axonal growth cone establishes a dynamic gradient of L1 adhesivity necessary to move along the substrate (Kamiguchi and Lemmon, 2000b). Indeed, such a gradient was recently detected and its maintenance was dependent on endocytic trafficking (Kamiguchi and Yoshihara, 2001). Our results suggest that the TI-VAMP–dependent intracellular trafficking of L1 may be necessary to stabilize and regulate adhesive contacts of neuronal cells. Clearly, the demonstration that TI-VAMP is an essential molecular player involved in the trafficking of L1 will greatly facilitate the analysis of the complex function and regulation of this highly important molecule in brain development.

The functional cross talk between TI-VAMP and L1 is highlighted by our finding that L1-mediated adhesion triggers the accumulation of TI-VAMP and L1-containing vesicles at the site of contact. The novelty of this finding raises several important questions. Are these vesicles involved in the establishment and/or maintenance of the contacts? Recent results on the regulation of L1-trafficking show that endocytosis of L1 is directly linked to tyrosine dephosphorylation of neuronal L1 on the YRSLE-motif (Schaefer *et al.*, 2002). Interestingly, this dephosphorylation seems to occur locally at sites where L1 is engaged in cell-cell contacts or axonal outgrowth on L1 substrate (Schaefer *et al.*, 2002). The concentration of TI-VAMP vesicles at L1-dependent contacts might therefore provide the trafficking machinery necessary for L1 to recycle locally and thus perform its function. How does L1-dependent signaling control membrane trafficking? Activation of L1 by homophilic interaction stimulates a signaling pathway involving src, PI3Kinase, Rac1, and the mitogen-activated protein kinases, and activation of src seems to play an essential role in L1-dependent neurite outgrowth (Ignelzi *et al.*, 1994; Schaefer *et al.*, 1999; Schmid *et al.*, 2000). Also, L1 interacts directly with scaffolding proteins such as Ankyrin and Ezrin (Davis and Bennett, 1994; Dickson *et al.*, 2002). Future studies should test how far the recruitment of TI-VAMP vesicles to L1-dependent contacts depends on any of the proteins mentioned above or whether an as yet unknown mechanism is recruiting and stabilizing TI-VAMP vesicles.

Our findings have important implications for our understanding of the role of adhesion molecules such as L1 in the differentiation of neurons and the development of the brain. We propose that the function of L1 does not solely depend on its capacity to transduce intracellular signals and to mediate cell-to-cell adhesion but also consists in the targeting of the exocytic organelles involved in neurite outgrowth to the leading edge of growing axons and to sites of contact formation between cells. In light of the recent finding that N-CAM promotes the accumulation of *trans*-Golgi network organelles at sites of cell-cell contacts, a process that may activate the formation of synapses (Sytnyk *et al.*, 2002) and the link between TI-VAMP–mediated trafficking and L1-mediated adhesion unraveled herein, we propose that cross talk between membrane trafficking and cell-cell and cell-matrix adhesion molecules may be crucial for neuronal differentiation.

ACKNOWLEDGMENTS

REFERENCES

Advani, R.J., Yang, B., Prekeris, R., Lee, K.C., Klumperman, J., and Scheller, R.H. (1999). VAMP-7 mediates vesicular transport from endosomes to lysosomes. J. Cell Biol. *146*, 765–775.

Berditchevski, F. (2001). Complexes of tetraspanins with integrins: more than meets the eye. J. Cell Sci. *114*, 4143–4151.

Bogdanovic, A., Bennett, N., Kieffer, S., Louwagie, M., Morio, T., Garin, J., Satre, M., and Bruckert, F. (2002). Syntaxin 7, Syntaxin 8, Vti1 and VAMP7 form an active SNARE complex for early macropinocytic compartment fusion in *Dictyostelium discoideum*. Biochem J. *368*, 29–39.

Borgonovo, B., Cocucci, E., Racchetti, G., Podini, P., Bachi, A., and Meldolesi, J. (2002). Regulated exocytosis: a novel, widely expressed system. Nat. Cell Biol. *4*, 955–962.

Brummendorf, T., Kenwrick, S., and Rathjen, F.G. (1998). Neural cell recognition molecule L *1*, from cell biology to human hereditary brain malformations. Curr. Opin. Neurobiol. *8*, 87–97.

Chang, S., and De Camilli, P. (2001). Glutamate regulates actin-based motility in axonal filopodia. Nat. Neurosci. *4*, 787–793.

Chen, D., Minger, S.L., Honer, W.G., and Whiteheart, S.W. (1999). Organization of the secretory machinery in the rodent brain: distribution of the t-SNAREs, SNAP-25 and SNAP-23. Brain Res. *831*, 11–24.

Chilcote, T.J., Galli, T., Mundigl, O., Edelmann, L., McPherson, P.S., Takei, K., and De Camilli, P. (1995). Cellubrevin and synaptobrevins: similar subcellular localization and biochemical properties in PC12 cells. J. Cell Biol. *129*, 219–231.

Coco, S., Raposo, G., Martinez, S., Fontaine, J.J., Takamori, S., Zahraoui, A., Jahn, R., Matteoli, M., Louvard, D., and Galli, T. (1999). Subcellular localization of tetanus neurotoxin-insensitive vesicle-associated membrane protein (VAMP)/VAMP7 in neuronal cells: evidence for a novel membrane compartment. J. Neurosci. *19*, 9803–9812.

Dahme, M., Bartsch, U., Martini, R., Anliker, B., Schachner, M., and Mantei, N. (1997). Disruption of the mouse L1 gene leads to malformations of the nervous system. Nat. Genet. *17*, 346–349.

Davis, J.Q., and Bennett, V. (1994). Ankyrin binding activity shared by the neurofascin/L1/NrCAM family of nervous system cell adhesion molecules. J. Biol. Chem. *269*, 27163–27166.

De Angelis, E., MacFarlane, J., Du, J.S., Yeo, G., Hicks, R., Rathjen, F.G., Kenwrick, S., and Brummendorf, T. (1999). Pathological missense mutations of neural cell adhesion molecule L1 affect homophilic and heterophilic binding activities. EMBO J. *18*, 4744–4753.

Dickson, T.C., Mintz, C.D., Benson, D.L., and Salton, S.R. (2002). Functional binding interaction identified between the axonal CAM L1 and members of the ERM family. J. Cell Biol. *157*, 1105–1112.

Elbashir, S.M., Harborth, J., Lendeckel, W., Yalcin, A., Weber, K., and Tuschl, T. (2001). Duplexes of 21-nucleotide RNAs mediate RNA interference in cultured mammalian cells. Nature *411*, 494–498.

Filippini, F., Rossi, V., Galli, T., Budillon, A., D'Urso, M., and D'Esposito, M. (2001). Longins: a new evolutionary conserved VAMP family sharing a novel SNARE domain. Trends Biochem. Sci. *26*, 407–409.

Futerman, A.H., and Banker, G.A. (1996). The economics of neurite outgrowth–the addition of new membrane to growing axons. Trends Neurosci. *19*, 144–149.

Galli, T., and Haucke, V. (2001). Cycling of synaptic vesicles: how far? How fast! Sci STKE *2001*, RE1. Available at http://stke.sciencemag.org/. Accessed September 11, 2003.

Galli, T., Zahraoui, A., Vaidyanathan, V.V., Raposo, G., Tian, J.M., Karin, M., Niemann, H., and Louvard, D. (1998). A novel tetanus neurotoxin-insensitive vesicle-associated membrane protein in SNARE complexes of the apical plasma membrane of epithelial cells. Mol. Biol. Cell *9*, 1437–1448.

Grosse, G., Grosse, J., Tapp, R., Kuchinke, J., Gorsleben, M., Fetter, I., HohneZell, B., Gratzl, M., and Bergmann, M. (1999). SNAP-25 requirement for dendritic growth of hippocampal neurons. J. Neurosci. Res. *56*, 539–546.

Harlow, E., and Lane, D. (1988). Antibodies: A Laboratory Manual. Cold Spring Harbor, NY: Cold Spring Harbor Laboratory.

Ignelzi, M.A., Jr., Miller, D.R., Soriano, P., and Maness, P.F. (1994). Impaired neurite outgrowth of src-minus cerebellar neurons on the cell adhesion molecule L1. Neuron *12*, 873–884.

Kamiguchi, H., and Lemmon, V. (2000a). IgCAMs: bidirectional signals underlying neurite growth. Curr. Opin. Cell Biol. *12*, 598–605.

Kamiguchi, H., and Lemmon, V. (2000b). Recycling of the cell adhesion molecule L1 in axonal growth cones. J. Neurosci. *20*, 3676–3686.

Kamiguchi, H., Long, K.E., Pendergast, M., Schaefer, A.W., Rapoport, I., Kirchhausen, T., and Lemmon, V. (1998). The neural cell adhesion molecule L1 interacts with the AP-2 adaptor and is endocytosed via the clathrin-mediated pathway. J. Neurosci. *18*, 5311–5321.

Kamiguchi, H., and Yoshihara, F. (2001). The role of endocytic l1 trafficking in polarized adhesion and migration of nerve growth cones. J. Neurosci. *21*, 9194–9203.

Laemmli, U.K. (1970). Cleavage of structural proteins during the assembly of the head of bacteriophage T4. Nature *227*, 680–685.

Lambert, M., Padilla, F., and Mege, R.M. (2000). Immobilized dimers of N-cadherin-Fc chimera mimic cadherin-mediated cell contact formation: contribution of both outside-in and inside-out signals. J. Cell Sci. *113*, 2207–2219.

Le, T.L., Yap, A.S., and Stow, J.L. (1999). Recycling of E-cadherin: a potential mechanism for regulating cadherin dynamics. J. Cell Biol. *146*, 219–232.

Lemmon, V., Farr, K.L., and Lagenaur, C. (1989). L1-mediated axon outgrowth occurs via a homophilic binding mechanism. Neuron *2*, 1597–1603.

Liljelund, P., Ghosh, P., and van den Pol, A.N. (1994). Expression of the neural axon adhesion molecule L1 in the developing and adult rat brain. J. Biol. Chem. *269*, 32886–32895.

Martinez-Arca, S., Rudge, R.E., Vacca, M., Camonis, J., Daviet, L., Formstecher, E., Hamburger, A., Filippini, F., D'Esposito, M., and Galli, T. (2003b). A novel dual mechanism controlling the localization and function of exocytic v-SNAREs. Proc. Nat. Acad. Sci. USA. *100*, 9011–9016.

Martinez-Arca, S., Alberts, P., Zahraoui, A., Louvard, D., and Galli, T. (2000). Role of tetanus neurotoxin insensitive vesicle-associated membrane protein (TI-VAMP) in vesicular transport mediating neurite outgrowth. J. Cell Biol. *149*, 889–899.

Martinez-Arca, S., Coco, S., Mainguy, G., Schenk, U., Alberts, P., Bouille, P., Mezzina, M., Prochiantz, A., Matteoli, M., Louvard, D., and Galli, T. (2001). A common exocytotic mechanism mediates axonal and dendritic outgrowth. J. Neurosci. *21*, 3830–3838.

Martinez-Arca, S., Proux-Gillardeaux, V., Alberts, P., Louvard, D., and Galli, T. (2003a). Ectopic expression of syntaxin 1 in the ER redirects TI-VAMP- and cellubrevin-containing vesicles. J. Cell Sci. *116*, 2805–2816.

Mechtersheimer, S., Gutwein, P., Agmon-Levin, N., Stoeck, A., Oleszewski, M., Riedle, S., Fogel, M., Lemmon, V., and Altevogt, P. (2001). Ectodomain shedding of L1 adhesion molecule promotes cell migration by autocrine binding to integrins. J. Cell Biol. *155*, 661–673.

Muzerelle, A., Alberts, P., Martinez Arca, S., Jeannequin, O., Lafaye, P., Mazié, J.-C., Galli, T., and Gaspar, P. (2003). Identification of a presynaptic membrane compartment containing tetanus neurotoxin-insensitive vesicle associated membrane protein in the rat brain. Neuroscience. (*in press*).

Osen-Sand, A., Catsicas, M., Staple, J.K., Jones, K.A., Ayala, G., Knowles, J., Grenningloh, G., and Catsicas, S. (1993). Inhibition of axonal growth by SNAP-25 antisense oligonucleotides in vitro and in vivo. Nature *364*, 445–448.

Osen-Sand, A., Staple, J.K., Naldi, E., Schiavo, G., Rossetto, O., Petitpierre, S., Malgaroli, A., Montecucco, C., and Catsicas, S. (1996). Common and distinct fusion proteins in axonal growth and transmitter release. J. Comp. Neurol. *367*, 222–234.

Prochiantz, A. (1995). Neuronal polarity: giving neurons heads and tails. Neuron *15*, 743–746.

Rathjen, F.G., and Rutishauser, U. (1984). Comparison of two cell surface molecules involved in neural cell adhesion. EMBO J. *3*, 461–465.

Rousselet, A., Autillo-Touati, A., Araud, D., and Prochiantz, A. (1990). In vitro regulation of neuronal morphogenesis and polarity by astrocyte-derived factors. Dev. Biol. *137*, 33–45.

Schaefer, A.W., Kamei, Y., Kamiguchi, H., Wong, E.V., Rapoport, I., Kirchhausen, T., Beach, C.M., Landreth, G., Lemmon, S.K., and Lemmon, V. (2002). L1 endocytosis is controlled by a phosphorylation-dephosphorylation cycle stimulated by outside-in signaling by L1. J. Cell Biol. *157*, 1223–1232.

Schaefer, A.W., Kamiguchi, H., Wong, E.V., Beach, C.M., Landreth, G., and Lemmon, V. (1999). Activation of the MAPK signal cascade by the neural cell adhesion molecule L1 requires L1 internalization. J. Biol. Chem. *274*, 37965–37973.

Schagger, H., and von Jagow, G. (1987). Tricine-sodium dodecyl sulfate-polyacrylamide gel electrophoresis for the separation of proteins in the range from 1 to 100 kDa. Anal. Biochem. *166*, 368–379.

Schmid, R.S., Pruitt, W.M., and Maness, P.F. (2000). A MAP kinase-signaling pathway mediates neurite outgrowth on L1 and requires Src-dependent endocytosis. J. Neurosci. *20*, 4177–4188.

Schoch, S., Deak, F., Konigstorfer, A., Mozhayeva, M., Sara, Y., Sudhof, T.C., and Kavalali, E.T. (2001). SNARE function analyzed in synaptobrevin/VAMP knockout mice. Science *294*, 1117–1122.

Silletti, S., Mei, F., Sheppard, D., and Montgomery, A.M. (2000). Plasmin-sensitive dibasic sequences in the third fibronectin-like domain of L1-cell adhesion molecule (CAM) facilitate homomultimerization and concomitant integrin recruitment. J. Cell Biol. *149*, 1485–1502.

Sytnyk, V., Leshchynska, I., Delling, M., Dityateva, G., Dityatev, A., and Schachner, M. (2002). Neural cell adhesion molecule promotes accumulation of TGN organelles at sites of neuron-to-neuron contacts. J. Cell Biol. *159*, 649–661.

Verhage, M., *et al*. (2000). Synaptic assembly of the brain in the absence of neurotransmitter secretion. Science *287*, 864–869.

Wade, N., Bryant, N.J., Connolly, L.M., Simpson, R.J., Luzio, J.P., Piper, R.C., and James, D.E. (2001). Syntaxin 7 complexes with mouse Vps10p tail interactor 1b, Syntaxin 6, vesicle-associated membrane protein (VAMP)8, and VAMP7 in B16 melanoma cells. J. Biol. Chem. *276*, 19820–19827.

Washbourne, P., *et al*. (2002). Genetic ablation of the t-SNARE SNAP-25 distinguishes mechanisms of neuroexocytosis. Nat. Neurosci. *5*, 19–26.

Yang, B., Gonzalez, L., Prekeris, R., Steegmaier, M., Advani, R.J., and Scheller, R.H. (1999). SNARE interactions are not selective - Implications for membrane fusion specificity. J. Biol. Chem. *274*, 5649–5653.

Yip, P.M., and Siu, C.H. (2001). PC12 cells utilize the homophilic binding site of L1 for cell-cell adhesion but L1-alphavbeta3 interaction for neurite outgrowth. J. Neurochem. *76*, 1552–1564.